Short Papers

Equivalent Circuit Parameters of Microstrip Step Change in Width and Cross Junctions

A. GOPINATH, A. F. THOMSON, AND I. M. STEPHENSON

***Abstract*—The inductive component of the equivalent circuit of microstrip step change in width and cross junctions has been evaluated theoretically and a comprehensive set of results is presented. Experimental results for one set of step changes in width obtained using the resonant method compare well with theory.**

In an earlier paper [1] a method of calculating microstrip discontinuity inductances was developed. However, at the time of publication, detailed results for the step-width change and cross discontinuities were not available. Using the same method and computer program a comprehensive set of results has now been compiled for these discontinuities and is presented here. The capacitance components of the equivalent circuits for these discontinuities have been calculated by other authors [2], [3] and are available in the literature.

The first discontinuity considered here is the step change in width of microstrip lines. The layout of the discontinuity is given in Fig. 1(a) with the reference plane being set QQ'. For the sake of the calculation the excess current is assumed to be zero outside the region enclosed by NN' and MM'. The distances from NN' and QQ' and MM' to QQ' of $w_1/2$ and $w_2/2$, respectively, were used in calculation of results presented here. For some specific changes in width, lengths (NN' to QQ' and MM' to QQ') larger than those mentioned were used with little change in calculated results. From the previous paper

$$\Delta L = \int_{S_T}\int_{S_T} G_i \bar{J}_e \cdot \bar{J}_e \, dS \, dS' + \int_{S_1}\int_{S_T} G_i \bar{J}_e \cdot \bar{J}_{\infty w_1} \, dS \, dS'$$
$$+ \int_{S_2}\int_{S_T} G_i \bar{J}_e \cdot \bar{J}_{\infty w_2} \cdot dS \, dS' + \int_{S_T}\int_{w_1} G_1 \bar{J}_{\infty w_1} \cdot \bar{J}_e \, dy \, dS'$$
$$+ \int_{S_T}\int_{w_2} G_2 \bar{J}_{\infty w_2} \cdot \bar{J}_e \, dy \, dS' + \left(\int_{S_2}\int_{w_1} G_1 \bar{J}_{\infty w_1} \cdot \bar{J}_{\infty w_2} \, dy \, dS' \right.$$
$$\left. + \int_{S_1}\int_{w_2} G_2 \bar{J}_{\infty w_2} \cdot J_{\infty w_1} \, dy \, dS' - L_{-\infty w_2/2} - L_{-\infty w_1/2} \right)$$

where

S_T	region between NN' and MM';
S_1	from NN' to QQ';
S_2	QQ' to MM';
J_e	circulating current in the region S_T;
$J_{\infty w_1}, J_{\infty w_2}$	current distributions in uniform lines of widths w_1 and w_2, respectively.

$$G_i = \frac{1}{4\pi[(x-x_0)^2 + (y-y_0)^2]^{1/2}} - \frac{1}{4\pi[(x-x_0)^2 + (y-y_0)^2 + 4h^2]^{1/2}}$$

Manuscript received June 11, 1975; revised August 20, 1975. This work was supported by the Science Research Council, U. K., and one of the authors (A. F. T.) held a Science Research Council studentship during the course of this work.

The authors are with the School of Electronic Engineering Science, University College of North Wales, Bangor, Gwynedd, LL57 1UT Wales, U. K.

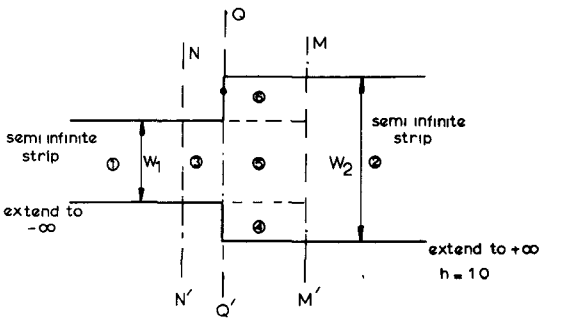

(a)

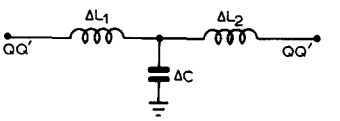

(b)

Fig. 1. (a) The step change in width showing the position of the reference plane QQ' and the rectangle elements used in the calculation. (b) Equivalent circuit of the step change in width. The calculations in this short paper give $\Delta L_1 + \Delta L_2$.

$$G_1 = \frac{1}{4\pi} \log_e \frac{(x-x_0) + \{(x-x_0)^2 + (y-y_0)^2 + (2h)^2\}^{1/2}}{(x-x_0) + \{(x-x_0)^2 + (y-y_0)^2\}^{1/2}}$$

and

$$G_2 = \frac{1}{4\pi} \log_e \frac{(x_0-x) + \{(x_0-x)^2 + (y_0-y)^2 + (2h)^2\}^{1/2}}{(x_0-x) + \{(x_0-x)^2 + (y_0-y)^2\}^{1/2}}$$

G_i, G_1, G_2 are the appropriate Green's function for the observation point $P(x,y,0)$ and termination point of the semi-infinite line at $(x_0,y_0,0)$.

$L_{-\infty w_1/2}$ and $L_{-\infty w_2/2}$ are differences in inductance between a semi-infinite line l long from the termination point of the semi-infinite line, and that of length l m, of infinite line, of widths w_1, w_2, respectively.

The terms in brackets can be calculated separately since $J_{\infty w_1}$ and $J_{\infty w_2}$, the current distributions, are known for infinite lines.

The equivalent circuit of discontinuity is given in Fig. 1(b). The ΔL calculated by the program is equal to the sum of ΔL_1 and ΔL_2, and the results obtained are shown in Fig. 2.

Experimental measurements for the step change were performed on straight-through resonators with the end effect appropriately calibrated as discussed by Easter [4].

The steps were placed at a zero-voltage point of a resonator, thus the shunt susceptance associated with the step had no effect. To avoid the necessity for measuring accurately the end and gap effects of lines of a variety of widths, the configuration of Fig. 3 was used. The two $\lambda/4$ end sections were both 50-Ω lines ($w/h = 1.0$), and the equivalent inductance of the steps was to be found from the measured resonant frequency of the test piece. The results are tabulated in Table I.

The normalized parameter $\Delta L/L_{\infty w_1} h$ is included since this was the parameter in the theoretical work. The theoretical and experimental results are compared in Fig. 4 and agreement is good.

On a set of 4 substrates with nominally identical test sections, the measured values of ΔL were within a range of ±5 percent. The absolute values of ΔL also depend on the accuracy to which the end and gap effects are measured which is ±5 μm, this represents an inductance error of $\pm 0.2 \times 10^{-11}$ H. The overall error is estimated at $\pm 0.3 \times 10^{-11}$ H and is shown as bars in Fig. 4.

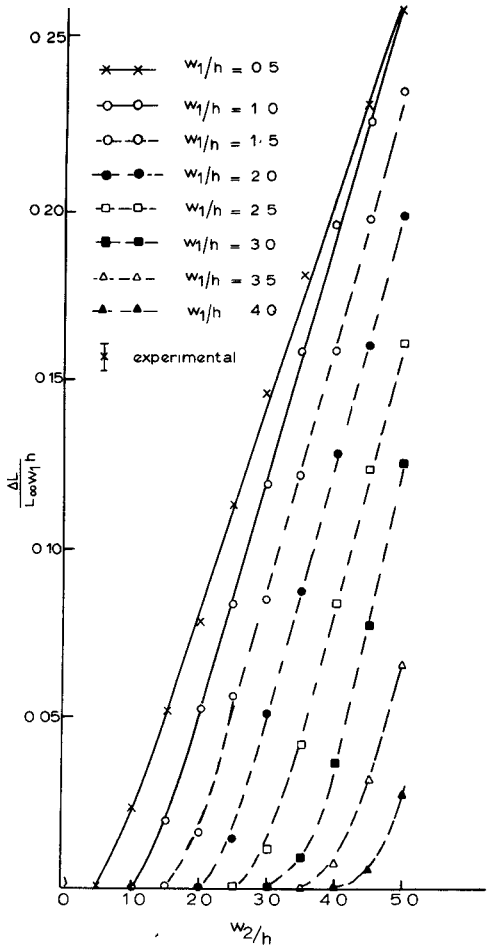

Fig. 2. The calculated inductance ΔL normalized to $L_{\omega w_1 h}$ for the equivalent circuit of step change in width of microstrip line.

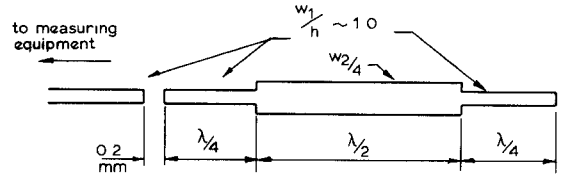

Fig. 3. Resonator configuration used for measuring step change in width of microstrip line on 0.637-mm alumina substrate.

TABLE I
MEASURED STEP CHANGES IN WIDTH INDUCTANCE GIVING INDUCTANCE AND FREQUENCY AT WHICH MEASUREMENT IS PERFORMED AT $w_1/h = 1.0$

w_2/h	Z_{02}	Step inductance ΔL	$L/L_{\omega w_1 h}$	Measurement frequency
2.0	33Ω	1.4×10^{-11} H	0.049	10 GHz
3.24	25Ω	3.1×10^{-11} H	0.11	7.5 GHz
4.0	21Ω	6.0×10^{-11} H	0.21	6.8 GHz
5.0	18.5Ω	8.0×10^{-11} H	0.28	6.8 GHz
6.0	16Ω	9.6×10^{-11} H	0.33	6.7 GHz

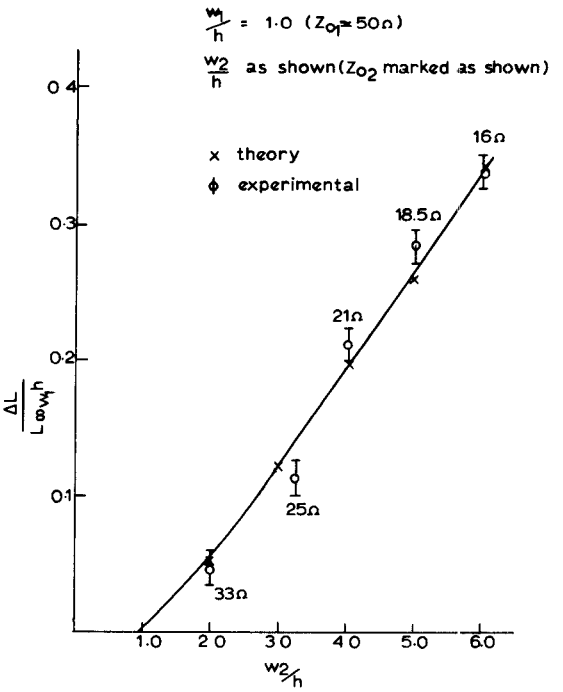

Fig. 4. Comparison between experimental and theoretical results for $w/h = 1.0$. Error bars indicate measurement accuracy, and the measured frequency values are give in Table I.

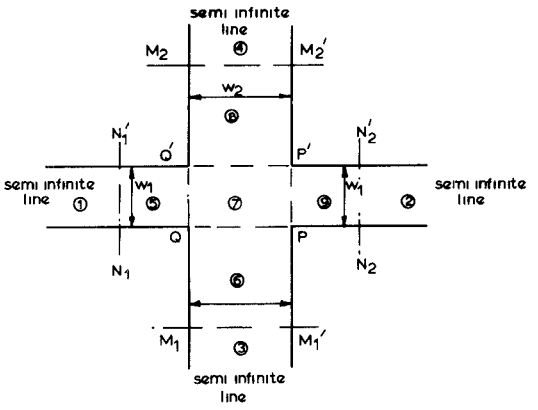

Fig. 5. (a) Symmetric cross junctions showing position of reference planes QQ', PP', QP, and $Q'P'$ and the rectangular elements used in the calculation. (b) Equivalent circuit of junction.

The second discontinuity investigated is the cross, but here again the only cases considered are where some symmetry exists, when the straight-through arms have the same width. Fig. 5(a) shows the geometry of the cross with appropriate reference planes and Fig. 5(b) shows the equivalent circuit proposed by Easter [4]. Note that this is somewhat different from that given by Silvester and Benedek [2], and at the present time it is not clear whether this four-capacitance configuration or a possible two-capacitance form is the most suitable. The layout of the discontinuity is given in

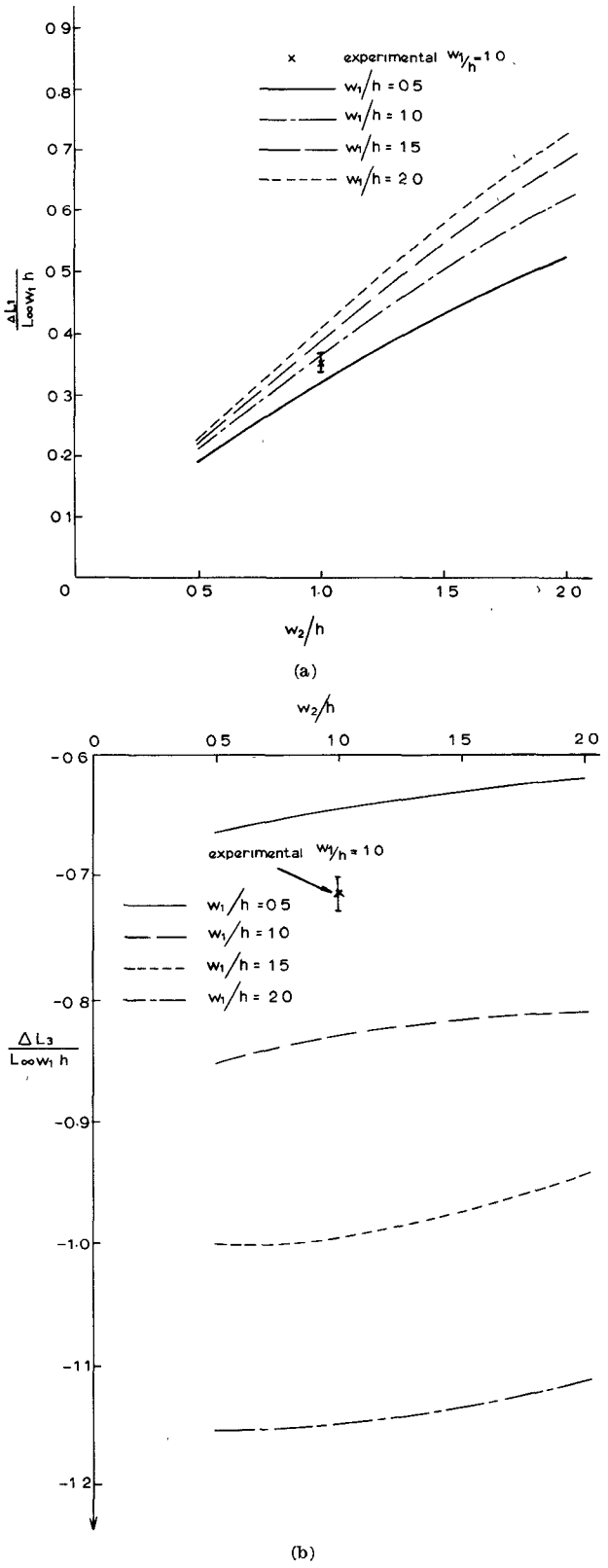

Fig. 6. (a) Calculated value of ΔL_1 normalized to $L_{\infty w1}h$ of the cross junction for different w_1/h and w_2/h. This same set of curves is to be used for estimating normalized ΔL_2. (b) Calculated value of ΔL_3 normalized to $L_{\infty w1}h$ of the cross junction.

Fig. 5(a) with reference planes at QQ', PP', QP, and $Q'P'$. As in the step, the excess current is assumed to be zero outside the area enclosed by the secondary references plane M_1M_1', M_2M_2', N_1N_1', and N_2N_2'. The distance from M_1M_1' to QQ' (and similar distances) was chosen so that the discontinuity inductance was not affected by any increase in this length. The results are summarized in Fig. 6(a) and (b) for different straight-arm ratios. Fig. 6(a) may also be used to evaluate the second inductance by turning the cross by 90°. Only one experimental point due to Easter [4] is available, and comparison with this theory shows that agreement is good for ΔL_1 and ΔL_2, but not for ΔL_3. Again, the disagreement in ΔL_3 is of the same order as our earlier results [1] for the T junction. The straight-through results of step change in width, straight arms of the T, and now the straight arms of the cross give very good agreement with experimental results. The theoretical results when the current goes around corners give poorer agreement with experiment. We may only conclude that the trial functions do not describe the current distribution adequately in these cases.

ACKNOWLEDGMENT

The authors wish to thank B. Easter for help and advice during this work.

REFERENCES

[1] A. F. Thomson and A. Gopinath, "Calculation of microstrip discontinuity inductances," *IEEE Trans. Microwave Theory Tech.*, vol. MTT-23, pp. 648–655, Aug. 1975.
[2] P. Silvester and P. Benedek, "Microstrip discontinuity capacitances for right-angle bends, T junctions, and crossings," *IEEE Trans. Microwave Theory Tech.*, vol. MTT-21, pp. 341–346, May 1973.
[3] A. Farrar and A. T. Adams, "Matrix methods for microstrip three-dimensional problems," *IEEE Trans. Microwave Theory Tech.*, vol. MTT-20, pp. 497–504, Aug. 1972.
[4] B. Easter, "Equivalent circuits of some microstrip discontinuities," *IEEE Trans. Microwave Theory Tech.*, vol. MTT-23, pp. 655–660, Aug. 1975.

A New Integrated Waveguide–Microstrip Transition

J. H. C. VAN HEUVEN, MEMBER, IEEE

***Abstract*—A new waveguide–microstrip transition is described. This design provides wide-band performance (18–26 GHz) and very good reproducibility without the need for variable elements. The circuit is fully integrated on the substrate and the characteristics are much less sensitive to small variations in the dimensions than other known transitions. A narrow-band version has been made for the telecommunication band in particular (17.7–19.7 GHz) with a VSWR less than 1.1 and an attenuation less than 0.25 dB.**

The design can easily be scaled to other frequencies and is especially useful at frequencies above 10 GHz.

INTRODUCTION

The introduction of MIC's in systems created the need for transitions between the conventional transmission lines and microstrip. At lower frequencies (below 10 GHz) a miniature coaxial connector is frequently used for this purpose.

The main problems are to establish a reliable contact between the inner conductor of the connector and the microstrip and to achieve adequate sealing of the circuit. Above 10 GHz such a transition is not satisfactory for most applications. Since many systems at these frequencies require waveguide components (e.g., low-loss filters, antenna horns) a direct waveguide–microstrip transition would be preferable and could solve the contact and sealing prob-

Manuscript received May 29, 1975; revised August 26, 1975.
The author is with the Philips Research Laboratories, Eindhoven, The Netherlands.